Predicting Fluid Flow in Gas-Stirred Systems

T. Deb Roy
The Pennsylvania State University
University Park, Pennsylvania

A. K. Majumdar
CHAM of North America Inc.
Huntsville, Alabama

SUMMARY

Performance of many metallurgical operations where gas bubbles are injected into liquid baths, e.g., ladle degassing and desulfurization, is related to the level of bath circulation and agitation. This paper describes a method of calculating velocity fields and turbulence levels in these systems. The roles played by such factors as bubble size and volume of the two-phase gas/liquid region in determining the velocity field are examined. The applicability of fluid-flow calculations in preventing refractory failures is discussed.

INTRODUCTION

There are many metal processing operations where gas bubbles are injected into liquid baths. Some examples of these operations are degassing of molten steel by injection of argon, desulfurization of steel baths by powder injection using inert carrier gases, and inert gas stirring of molten baths to achieve homogeneous temperature and composition. A schematic diagram of these systems is presented in Figure 1. In the central region of the vessel, a two-phase mixture, consisting of the injected gas bubbles and the melt, moves upward. The single-phase melt region, further away from the axis, also undergoes considerable circulation and agitation. Aspects of the metallurgical operations which are determined by the degassing or desulfurization time, or by the time needed to achieve homogeneous composition and temperature, are related to the details of the bath circulation (or velocity fields) and agitation (or turbulence levels).

Traditionally, the designer's need for understanding fluid-flow processes in the actual reactor has been met by performing model experiments. These experiments, while providing some useful qualitative description of the flow, suffer from two important limitations: 1) they are often expensive and time-consuming, and 2) it is impossible to achieve all the conditions of a real metallurgical process in a model.

A possible recourse is to calculate flow field and turbulence levels by solving a set of partial differential equations governing the transport of momentum, mass and other properties of the flow. However, unlike the single-phase laminar flow situations where numerical predictions are straightforward and can be as reliable as the measurements, flow prediction in metallurgical processes is much more complex. Realistic hydrodynamic calculations in many metallurgical systems involve treatment of two-phase turbulent recirculating flows with several special features. In metallurgical systems, gases may be injected through porous plugs, tuyeres, or nozzles. These various injection modes result in differences in bubble size, gas holdup, and the degree of slip between the gas bubbles and the melt. This paper outlines a calculation scheme which takes these factors into consideration. The reliability of the computation scheme is examined by comparing the predicted velocity fields with experimental data.

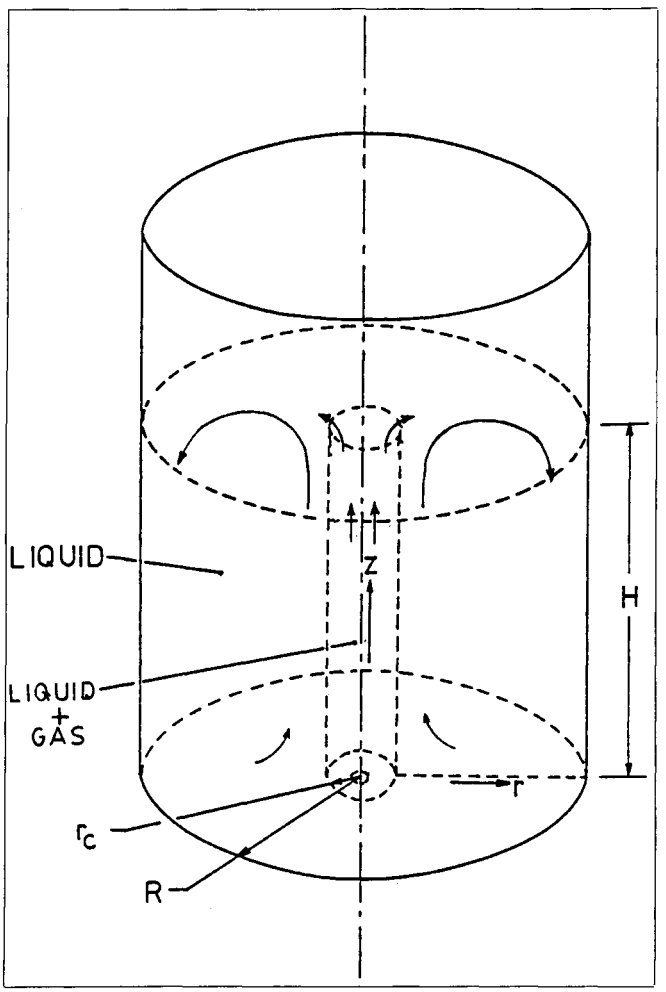

Figure 1. Schematic diagram of the gas-stirred reactor.

In gas-stirred systems, the boundary separating the recirculating liquid with the central core containing the two-phase gas liquid dispersion is not clearly defined. However, the size of the two-phase region is important. First, the knowledge of its size allows attention to be focused on the single-phase liquid metal region, thereby achieving considerable simplification. Second, information of the velocity field as affected by the size of the two-phase region can reveal significant insight into these processes.

Furthermore, the reliability of the flow pattern in metallurgical systems depends on the ability to model turbulence

in these systems. Since the quality of the predicted velocity profiles is affected by the choice of turbulence models, a selection of the computed results is presented to examine the sensitivity of the predicted velocity field on the selection of turbulence models. Apart from providing a basis for predicting overall performance characteristics of important metallurgical processes, the calculation of hydrodynamic variables also provides insight into the process.

MATHEMATICAL MODELING

Governing Equations

The equations used for flow prediction are the equation of continuity and the equation of motion in two dimensions. General forms of these equations for turbulent flow in cylindrical coordinates are well documented in standard textbooks and are not presented here. However, since the special feature of the computation lies in modifying the axial momentum equation, this equation is discussed. The modification is made in order to include the appropriate body-force term to account for the buoyancy force resulting from gas injection. Furthermore, since the gas bubbles do not move with the liquid phase at the same velocity, an allowance is made to account for the free convection of gas bubbles through the liquid phase. With reference to the coordinate system shown in Figure 1, the z-direction momentum equation is*

$$\frac{\partial}{\partial z}(\rho u^2) + \frac{1}{r}\frac{\partial}{\partial r}(\rho r v u) = -\frac{\partial p}{\partial z} + \frac{\partial}{\partial z}\left(\mu_{eff}\frac{\partial u}{\partial z}\right) + \frac{1}{r}\frac{\partial}{\partial r}\left(r\mu_{eff}\frac{\partial u}{\partial r}\right) + S_u \quad (1)$$

where:

$$S_u = \frac{\partial}{\partial z}\left(\mu_{eff}\frac{\partial u}{\partial z}\right) + \frac{1}{r}\frac{\partial}{\partial r}\left(\mu_{eff} r \frac{\partial v}{\partial r}\right) + \rho g \bar{\alpha} \quad (2)$$

where $\bar{\alpha}$ is the void fraction and $\rho g \bar{\alpha}$ is the source term representing the buoyancy force. The momentum equation includes two symbols: μ_{eff}, the effective viscosity and $\bar{\alpha}$, the void fraction, which are of crucial importance in determining the flow pattern. A discussion of the calculation schemes for these two quantities follows.

Calculating the Effective Viscosity

Unlike molecular viscosity, effective viscosity, μ_{eff}, is not a physical property of the liquid. Its value is related to the nature of the flow and the specific location inside the system where it is evaluated. The task of expressing effective viscosity in terms of known or calculable quantities is accomplished in two different ways. Effective viscosity is sometimes calculated from a simple algebraic formula involving system geometry and mean velocities. In relatively more sophisticated treatments, its value is determined by solving differential equations for one or more properties of turbulent motion. Calculations involving both these approaches are presented in this paper. The differential equation approach adopted in the present work involves solving two additional equations, one representing the conservation of turbulent kinetic energy (k) and the other dealing with the local dissipation rate of this energy (ϵ). These equations[3] and the boundary conditions for k and ϵ are presented in the appendix. The algebraic equation model used in this work is relatively simple and will be discussed subsequently in the text.

Calculating the Void Fraction

For the single-phase region far away from the central core, the void fraction is zero. In the two-phase region, the void fraction $\bar{\alpha}$ is estimated by using the following equation representing the mass balance on the gas phase.[1]

$$\bar{\alpha} = \frac{1}{2\pi}\,\frac{V_{gas}}{\int_0^{r_c} r(u + U_{slip})dr} \quad (3)$$

where U_{slip} is the velocity of slip between the gas and the liquid phase or the terminal velocity of the bubbles in the liquid. This velocity is determined by the physical properties of the gas and the liquid, and the size and type of the bubble (spherical cap or nearly spherical, etc.) In turn, the shape and size of bubbles are determined by the method in which the gas is injected, i.e., through a porous plug, a lance, or a nozzle. If the gas bubbles move at the same velocity with the liquid packet, U_{slip} is taken as zero. For the spherical cap bubbles, U_{slip} has been determined[2] to be about 40 cm/sec. It is noted that the void fraction $\bar{\alpha}$, as defined in Equation 3, is a function of axial distance and also depends on the choice of r_c, the radius of the two-phase gas/liquid dispersion column. The density ρ appearing in the momentum equation is expressed by the following equations:

$$\rho = (1 - \bar{\alpha})\rho_l, \text{ for } r < r_c \quad (4)$$

and

$$\rho = \rho_l, \text{ for } r \geq r_c \quad (5)$$

Boundary Conditions

The boundary conditions for solving the set of equations representing the equation of continuity and the equation of motion include a statement of symmetry about the vertical axis of the vessel. At the axis,

$$\left.\begin{aligned}\frac{\partial u}{\partial r} &= 0\\ v &= 0\end{aligned}\right\} \quad (6)$$

At the walls of the vessel both the axial and radial velocities are zero, i.e.,

$$u = v = 0 \quad (7)$$

The free surface is stable and therefore the time average axial velocity is zero. Furthermore, no shear stress is transmitted through the free surface. At the free surface,

$$\left.\begin{aligned}u &= 0\\ \frac{\partial v}{\partial z} &= 0\end{aligned}\right\} \quad (8)$$

The computational procedure used has been described in an earlier publication[1] and is not discussed here.

*Terms are identified in the Nomenclature at the end of this paper.

RESULTS AND DISCUSSION

Turbulence Modeling

It is interesting to note that some of the earlier works dealing with the prediction of fluid flow in gas-stirred metallurgical reactors have restricted the treatment to only the single-phase liquid region.[4] Such treatments, while requiring a prescription of measured velocity distribution at the gas/liquid interface ($r = r_c$ plane, Figure 1), have been simplified. In the present work, such simplification has been adopted only for examining the effects of alternate turbulence models on the quality of the predicted flow field. Much of the complexity in the prediction of turbulent recirculating flows in metallurgical reactors is due to turbulence modeling. Whether the use of a relatively simpler turbulence model compromises the accuracy of the predicted flow field critically is a significant question.

In Figure 2 the computed velocity profiles are presented for three different viscosity models for the experimental conditions of Szekely et al.[4] presented in Table I. The computations using a two equation model (Appendix) are shown in Figure 2a. Computations were also performed (Figure 2b) where the value of the effective viscosity was prescribed by the following relatively simple expression suggested by Pun and Spalding.[5]

$$\mu_{eff} = K(2R)^{2/3}(H)^{-1/3}\rho_l^{2/3}\,(m_j u_j^2)^{1/3} \qquad (9)$$

Where m_j is the mass flow rate of the gas, u_j is the gas velocity at the nozzle exit, and K is a constant whose value, according to Pun and Spalding,[5] is 0.012. For the experimental conditions presented in Table I, the value μ_{eff} has been found to be equal to 0.9 gm (cm/s).

Table I: Data for Experimental Situation Used by Szekely et al[4]

Vessel diameter	0.6 m
Water column height	0.6 m
Velocity of air through orifice	1.62 m
Orifice diameter	0.127 m
r_c/R	0.18

The velocity profiles of Figure 2c were calculated using laminar viscosity. A quantitative comparison of the predicted velocity distributions for these different viscosity values is presented in Figure 3. It is observed that the laminar flow model generates relatively less circulation in the reactor. This represents the fact that the motion in the reactor is largely due to shear flow. It is interesting to note that although the flow predictions by the above "ad-hoc" viscosity model (Equation 9) and the K-ϵ turbulence model (Appendix) exhibits similarity in most parts of the flow domain, the main differences appear in the "near-wall" regions. In the ad-hoc viscosity model, the predicted near-wall velocities are relatively smaller due to the presumption of large frictional effects in these regions. It is interesting to

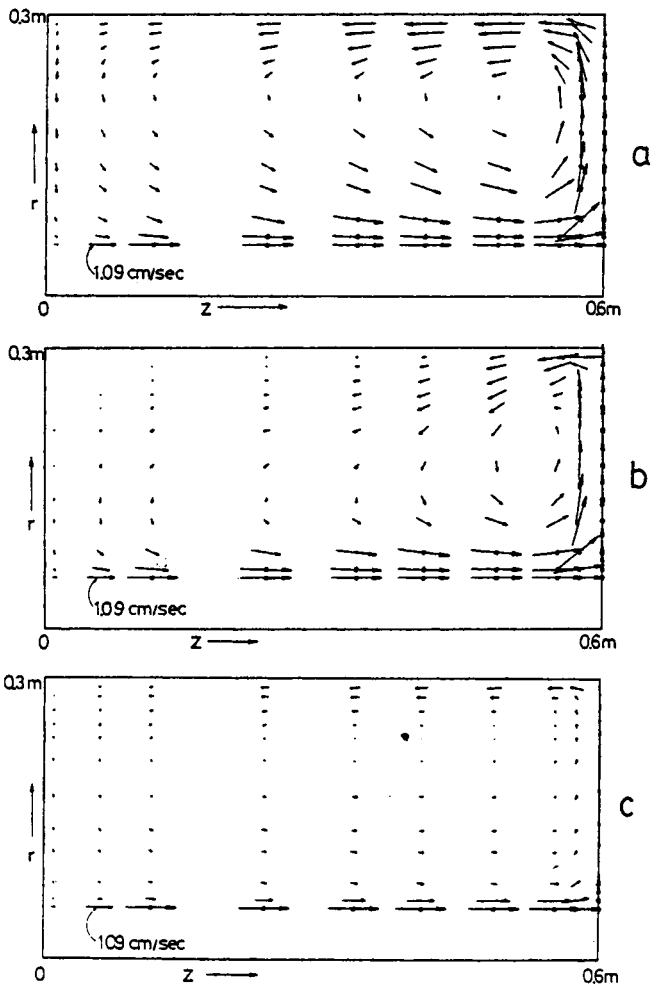

Figure 2. Predicted velocity fields for different effective viscosity values; (a) K-ϵ model, (b) effective viscosity model (Equation 3) and (c) laminar viscosity model. The symbol ➢ indicates that the velocity exceeds 0.2 m/s. Other data are listed in Table I.

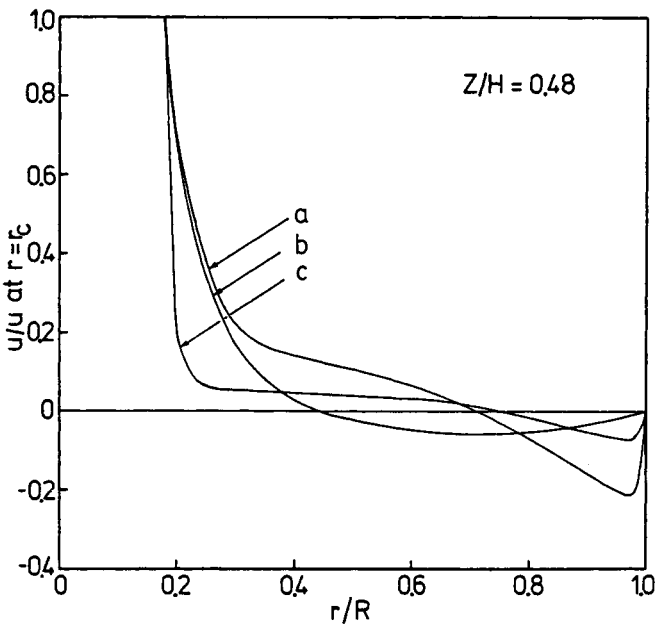

Figure 3. Quantitative comparison of the predicted u velocity distributions (also see Table I). Notations (a), (b) and (c) have the same meaning as Figure 2.

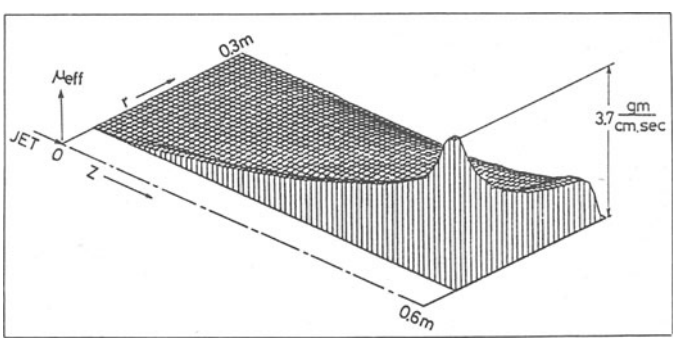

Figure 4. Computed values of effective viscosity.

note that if near-wall corrections are introduced it would be attractive to use Equation 9 to evaluate effective viscosity for the recirculating flow since it would significantly reduce the computational task.

The computed values of the effective viscosity are shown in Figure 4. It is observed that the maximum value of the effective viscosity is attained at the central region ($r = r_c$) near the free surface. The presence of high shear in this region is consistent with the fact that the fluid particles make a right-angle turn in this region.

Refractory Design Based on Fluid Flow Computations

In the last two decades, ladle metallurgical operations have become increasingly important in the overall operating schedule of the integrated iron and steel works. The service life of a refining ladle is determined by the life of its refractories. During refining, the refractory erosion in these processes results primarily from mechanical erosion caused by the turbulent liquid flow and the chemical erosion from reactions at the refractory/metal interface. Several of these reactions are controlled by mass transfer and, therefore, their rates can be related to local velocities or shear stresses.

Since the mechanical erosion due to turbulent flow depends on the local values of shear stress, the erosion is likely to be relatively high in the areas of higher shear stress. The predicted values of wall shear stress is shown in Figure 5. The maximum value of wall shear stress appears near the free surface ($Z/H = 0.9$). Fluid flow computations can reveal the locations where the refractory lining is most vulnerable to wear. Therefore, the computations provide a basis for taking appropriate preventive measures, such as designing the refractory lining to incorporate localized line thickening or using appropriate refractory material or material combinations at critical locations.

The Effect of the Volume of the Two-Phase Region

In the computed results presented so far, attention was focused only on the single-phase region. The effect of two-phase gas/liquid mixture was introduced by prescribing a measured velocity distribution at the gas/liquid interface ($r = r_c$). This requirement is not easy to meet for the analysis of high-temperature metallurgical processes such as degassing steel by argon injection. The results presented in the following sections were generated by using the fully predictive method discussed in the formulation section. Here the flow fields are generated by prescribing the gas flow rate and the bubble size. Also, since the ad-hoc viscosity model provided a reasonable prediction of the velocity field with very little computational costs, this model was used in the computations reported in this section and subsequently in this paper.

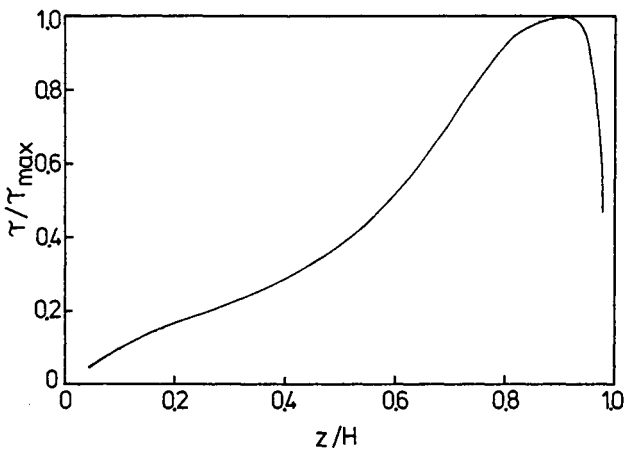

Figure 5. Predicted values of normalized wall shear stress.

In gas-stirred ladles, the transfer of impurities from the melt to the gas phase takes place in the two-phase region at the central region of the bath. Presumably the size of this zone depends on a number of factors such as the gas flow rate, the bath height, the physical properties of the liquid and the gas, the bubble size, etc. A parametric computation has been performed to investigate the influence of the volume of two-phase region on the predicted flow pattern. Predicted velocity profiles for three different values of r_c/R are shown in Figure 6. A significant variation of the predicted flow field is observed with the variation of r_c/R in the region close to the axis of the vessel ($r/R < 0.3$). However, in most parts of the flow domain away from the axis ($r/R > 0.3$), the variation of the predicted velocity field with the variation of r_c/R is insignificant.

The Effect of Bubble Size

For a given gas injection rate, the bubble size depends on the type of injection equipment, such as porous plugs, nozzles, and lances. The velocity of slip between the liquid and the gas phase can be correlated with the size of the bubbles. As pointed out earlier, the velocity of slip or the terminal velocity for the spherical cap bubbles has been experimentally determined by Davenport et al.[2] to be 40 cm/s. For smaller bubbles, the approximate value of the terminal velocity can be obtained by using the well-known

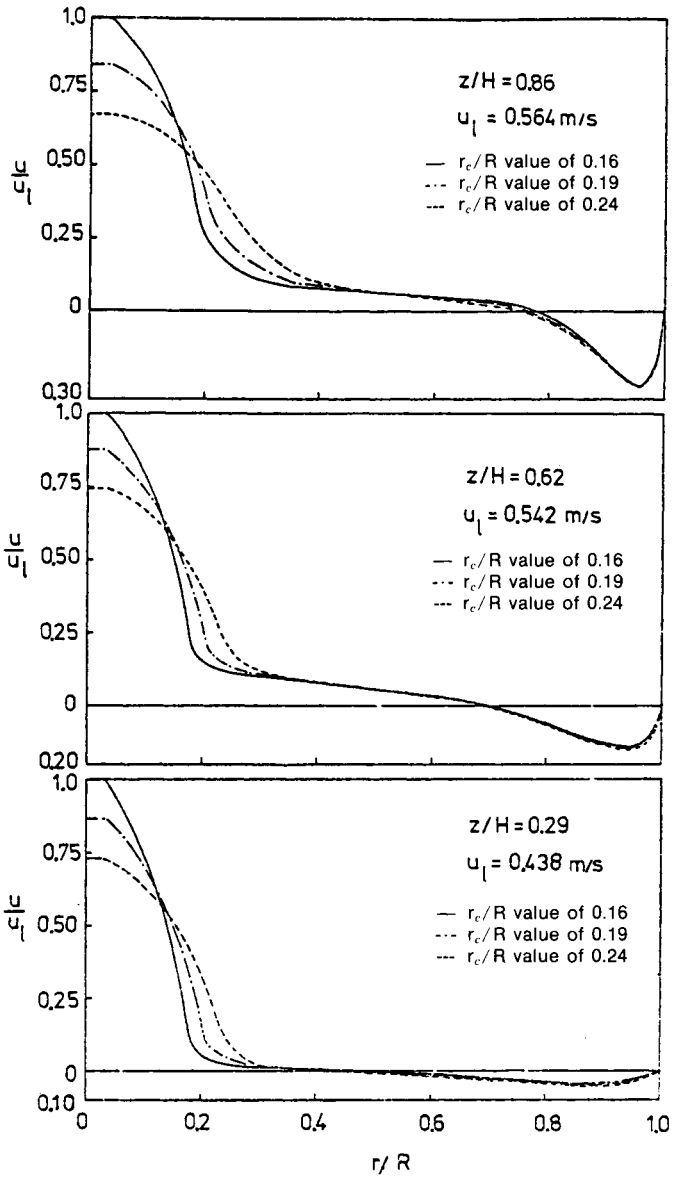

Figure 6. Quantitative comparison of the predicted u velocity distribution at difference values of z/H.

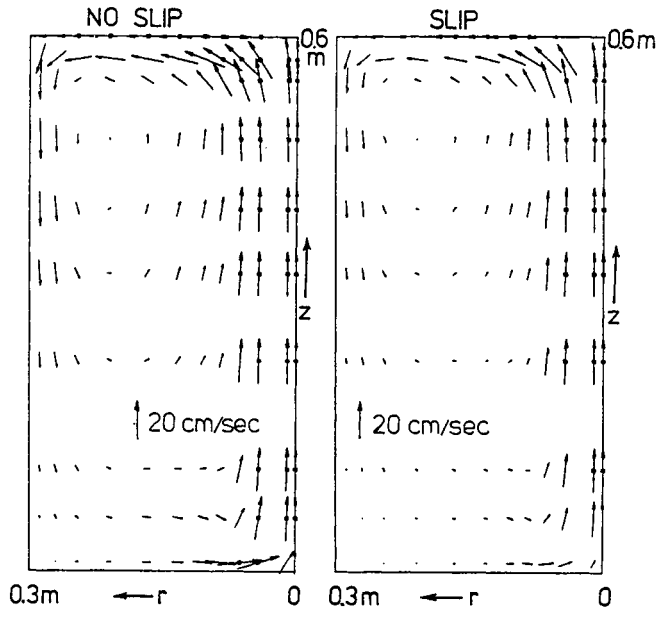

Figure 7. Predicted velocity fields for slip and no-slip conditions (r_c/R = 0.24). The symbol ➤ indicates that the magnitude of the velocity exceeds 20 cm/s.

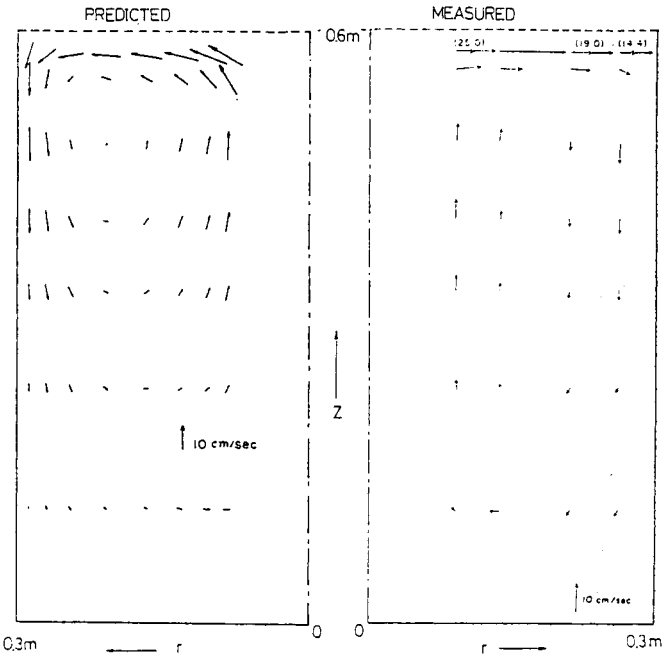

Figure 8. Experimental[4] (see Table I) and predicted (allowing for slip, r_c/R = 0.24) velocity fields.

Stokes Law. For very small bubbles, the terminal velocity (U_{slip}) is small, and the bubbles move at a velocity which is essentially the same as that of the liquid, thereby approaching a no-slip condition.

Figure 7 represents the computed velocity field for slip and no-slip (U_{slip}=0) cases. It may be noted that the no-slip model predicts relatively higher velocities in an otherwise identical situation. This observation is also realistic since the buoyancy effect is larger in the no-slip model due to larger gas holdup in the vessel.

Figure 8 provides a comparison between the predictions of velocity field with the slip model and the experimental measurements of Szekely et al.[4] A reasonable agreement is achieved between the measurements and the predicted values.

CONCLUDING REMARKS

A computation scheme is outlined for the calculation of hydrodynamic variables in gas-stirred metallurgical reactors. The novelty of the method is its ability to predict the difference in the fluid-flow field due to variations in bubble size and gas flow rate—a feature essential for the analysis of various metallurgical processes.

It is established that for the same volumetric flow rate of gas there can be considerable difference in the velocity field due to difference in bubble size. However, in most parts of the reactor away from the axis, the predicted velocity field is not affected by a variation in the size of the two-phase gas/liquid region. When the objective is to calculate the velocity field alone and the information on the level of turbulence is not required, an ad-hoc viscosity model can be conveniently used to predict the velocity field with reasonable accuracy and with very little computation cost.

While more accurate experimental measurements of hydrodynamic variables are needed in metallurgical systems, the present prediction capability can be used more extensively in metallurgical process analysis and modification with gratifying results.

References

1. T. Deb Roy, A. K. Majumdar and D. B. Spalding, **Appl. Math. Modelling, 2,** 1978, pp. 146-150.
2. W. G. Davenport, F. D. Richardson and A. V. Bradshaw, **J. Iron Steel Inst., 209,** 1967, p. 1034.
3. F. H. Harlow and P. I. Nakayama, Transport of Turbulence Energy Decay Rate, Los Alamos Sci. Lab, University of California, LA-3854, 1968.
4. J. Szekely, H. Y. Wang and K. M. Kiser, **Met. Trans. B, 7B,** 1976, pp. 287-295.
5. W. M. Pun and D. B. Spalding, Mich. Eng. Dept. Rep. SF/TN/11, 1967, Imperial College as quoted in A. D. Gosman et al. in "Heat and Mass Transfer in Recirculating Flows," Academic Press, London and New York, 1969.
6. B. E. Launder and D. B. Spalding, **Computer Methods in Appl. Mechanics and Engineering, 3,** 1974, pp. 269-289.

APPENDIX

In the majority of computations presented in this paper, the effective viscosity, μ_{eff} is calculated from a two-equation turbulence model. In this model the Reynolds stresses are related to the mean rate of strain through a turbulent viscosity which is determined by the local values of density, turbulence kinetic energy, k, and its dissipation rate, ϵ. The governing differential equations for k and ϵ are:

$$\text{Turbulence energy: } \frac{\partial}{\partial z}(\rho u k) + \frac{1}{r}\frac{\partial}{\partial r}(\rho r v k) = \frac{\partial}{\partial z}\left(\frac{\mu_{eff}}{\sigma_k}\frac{\partial k}{\partial z}\right) + \frac{1}{r}\frac{\partial}{\partial r}\left(r\frac{\mu_{eff}}{\sigma_k}\frac{\partial k}{\partial r}\right) + S_k \tag{A.1}$$

$$\text{where } S_k = G - \rho\epsilon \tag{A.2}$$

$$\text{and } G = \mu_t\left[2\left\{\left(\frac{\partial u}{\partial z}\right)^2 + \left(\frac{\partial v}{\partial r}\right)^2 + \left(\frac{v}{r}\right)^2\right\} + \left(\frac{\partial u}{\partial r} + \frac{\partial v}{\partial z}\right)^2\right] \tag{A.3}$$

Dissipation rate of turbulence energy:

$$\frac{\partial}{\partial z}(\rho u \epsilon) + \frac{1}{r}\frac{\partial}{\partial r}(\rho r v \epsilon) = \frac{\partial}{\partial z}\left(\frac{\mu_{eff}}{\sigma_\epsilon}\frac{\partial \epsilon}{\partial z}\right) + \frac{1}{r}\frac{\partial}{\partial r}\left(r\frac{\mu_{eff}}{\sigma_\epsilon}\frac{\partial \epsilon}{\partial r}\right) + S_\epsilon \tag{A.4}$$

and

$$S_\epsilon = \frac{C_1 \epsilon G}{k} - \frac{C_2 \rho \epsilon^2}{k} \tag{A.5}$$

The expression for μ_{eff} is

$$\mu_{eff} = \mu_l + C_D \rho k^2 / \epsilon \qquad (A.6)$$

The model contains five empirical constants which are assigned the following typical values:[6]

C_1	C_2	σ_k	σ_ϵ	C_D
1.43	1.92	1.0	1.3	0.09

The boundary conditions used for the turbulent quantities are the following. At the gas liquid interface ($r = r_c$) and at the free surfaced the gradients of k and ϵ are set to zero. At the solid walls the values of k and ϵ are zero.

NOMENCLATURE

C_1, C_2, and C_D	constants of K-ϵ model
g	acceleration due to gravity, m/s^2
G	defined by Equation A.2
H	height of liquid column in the vessel, m
K	constant, defined after Equation 9
k	turbulence kinetic energy, m^2/s^2
l	length-scale of turbulence, m
m_j	mass flow rate of gas, kg/s
p	pressure, kg/m-s^2
R	radius of the vessel, m
r	radial distance from the axis of symmetry, m
r_c	radius of the core (Figure 1)
S_k, S_u, and S_ϵ	source terms defined by Equations A.2, 2 and A.5, respectively
U_{slip}	velocity of slip between the gas and the the liquid phases, m/s
u	velocity in axial direction, m/s
u_j	inlet gas velocity, m/s
V_{gas}	volumetric flow rate of gas, m^3/s
v	velocity in radial direction, m/s
z	axial distance from the bottom of the vessel, m

Greek Symbols

$\overline{\alpha}$	void fraction defined by Equation 3
ϵ	dissipation rate of turbulence kinetic energy, m^2/m^3
μ_l	molecular viscosity, kg/m-s
μ_t	turbulent viscosity, kg/m-s
μ_{eff}	effective viscosity, kg/m-s
σ_k, σ_ϵ	effective Schmidt number of subscripted entity
τ	wall shear stress, kg/m-s^2
ρ	density of two phase mixture, kg/m^3
ρ_e	density of liquid, kg/m^3

ABOUT THE AUTHORS

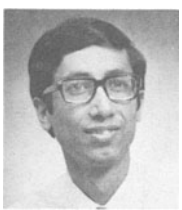

T. Deb Roy is assistant professor of metallurgy at the Pennsylvania State University where he teaches courses in the general area of Pyrometallurgy and Materials Processing. His research interests are in the areas of mathematical modeling of metallurgical processes, pyrometallurgy and welding. Previously, he was on the research staffs of MIT and Imperial College, England.

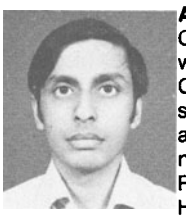

A. K. Majumdar is project engineer in CHAM of North America, Inc. Previously he worked in Imperial College, England and in Central Mechanical Engineering Research Institute, India. He obtained his bachelor's and master's degrees in mechanical engineering from University of Calcutta, and his PhD from University of Burdwan, India in 1974. His current area of interest is the mathematical modeling of fluid flow and heat transfer.

Government, Energy, and Materials (GEM) Affairs Washington Notes

(Continued from page 39)

(EN-336), Washington, D.C. 20460; telephone (202) 426-7025.

NSF Analyzes Industry Employment. In a recent study, the National Science Foundation found that science and engineering employment in private industry was virtually unchanged between 1978 and 1980, a decline in the manufacturing industries being offset by a gain in the service industries. Of the 2.1 million employed persons, almost one-half were technicians, and of the remaining 1.1 million, about 80% were engineers. Nonmanufacturing industries accounted for 40% of the 1980 employment, but accounted for 60% of that employment growth between 1978 and 1980. Copies of the report, "Scientists, Engineers, and Technicians in Private Industry, 1978-80," can be purchased from the Superintendent of Documents, GPO, Washington, D.C. 20402 (Stock No. 038-000-00472-7; $2.00); telephone (202) 783-3238.

BuMines Publishes Minerals Data Book. All three volumes of the latest "Minerals Yearbook," providing in-depth statistics on mineral production and consumption for the years 1978 and 1979, are now available. Volume I covers nonfuel minerals on an individual commodity basis. Volumes II and III cover the 50 states and foreign countries, respectively. All three volumes (Volume I, Stock No. 024-044-02021-1, $15.00; Volume II, Stock No. 024-004-02064-4, $12.00; Volume III, Stock No. 024-044-02066-1, $17.00) can be purchased from the Superintendent of Documents, GPO, Washington, D.C. 20402; telephone (202) 783-3238. Single copies of up to five individual chapters (by commodity, state, country) are available without charge from Publications Distribution, Bureau of Mines, 4800 Forbes Avenue, Pittsburgh, Pennsylvania 15213; telephone (412) 621-4500, extension 342.

GAO Completes Two Studies. In "Major Science and Technology Issues" (Acc. No. 11424 (PAD-81-35), 54 pp.), emerging issues related to federal involvement are identified. In "Possible Ways to Streamline Existing Federal Energy Mineral Leasing Rules" (Acc. No. 112316 (EMD-81-44), 48 pp.), inconsistences in federal leasing laws from one mineral to another are shown, and possible improvements in the system are described. Free single copies of these reports are available from U.S. General Accounting Office, Information Services Facility, Box 6015, Gaithersburg, Maryland 20760; telephone (301) 275-6241.